Eur. J. Mech. B - Fluids 20 (2001) 511–524

S0997-7546(01)01131-1/FLA

Thermal perturbation of trailing vortices

Paolo Orlandi [a], George F. Carnevale [b,*], S.K. Lele [c], K. Shariff [d]

[a] *Universita di Roma 'La Sapienza', Dipartimento di Meccanica e Aeronautica, via Eudossiana 18, 00184 Roma, Italy*
[b] *Scripps Institution of Oceanography, University of California San Diego, 9500 Gilman Dr., La Jolla, CA 92093, USA*
[c] *Department of Aeronautics and Astronautics, Stanford University, Stanford, CA 94305, USA*
[d] *NASA-Ames Research Center, Moffett Field, CA 94035, USA*

(Received 2 April 2000; accepted 20 September 2000)

Abstract – The possibility of diminishing the danger of trailing vortices through thermal forcing is investigated. It is shown that heating the vortices would have two beneficial effects. First, it would cause the vortices to descend more rapidly thus clearing the flight path more quickly. Second, it would cause the vortices to draw closer together, thus greatly increasing the growth rate of the short-wave instabilities that can ultimately destroy the vortices through cross-diffusion. © 2001 Éditions scientifiques et médicales Elsevier SAS

1. Introduction

Vortices in the wake of heavy aircraft pose a serious threat to following aircraft. The danger is particularly severe during landings and takeoffs for two reasons: the extension of the flaps of the leading aircraft may create trailing vortices that are even stronger than the wing tip vortices and the proximity of the following aircraft to the ground means that a small perturbation in its trajectory may be disastrous. The current strategy for dealing with this problem involves simply allowing sufficient time between landings and takeoffs. This scheme relies essentially on two mechanisms that lessen the dangers of the trailing vortices. The first is that the vortices advect each other out of the flight path of the following plane (Rennich [1]). This is possible because the vortices come in counter-rotating pairs oriented in such a way that they propagate downward. This effect alone is not sufficient to eliminate the problem on runways because the vortices are not destroyed when they hit the runway but rebound and interact in a complicated way that does not ensure there dispersal (Orlandi [2]; Spalart [3]). Thus, near the runway, secondary effects must come into play to diminish the threat of these vortices. For example, cross winds can move the vortices laterally away from the runway. But the actual destruction of the vortices only comes about through vortex instabilities that ensue when vortices come close together. These instabilities of the two vortex system are initiated by ambient turbulence (Spalart [3]) and mix the opposite signed vorticity together destroying the strength of the vortices in a process called cross-diffusion. If the trailing vortices could be brought closer together this would at once increase the speed at which they leave the flight path and promote instabilities that eventually result in their destruction. This may be accomplished through the effect of heating the vortices as we will discuss below.

Before dealing with the effect of thermal forcing, we will review some of the relevant issues regarding the use of vortex instabilities to accelerate vortex decay. To be explicit in the discussion, we will refer to the schematic

* Correspondence and reprints.
E-mail address: gcarnevale@ucsd.edu (G.F. Carnevale).

diagram in *figure 1*. Trailing vortices come in counter-rotating pairs. The wing tips of the plane each shed one vortex in such a pair. Also the flaps when extended shed pairs of vortices. The diagram in *figure 1* shows the separation distance b between the centers of the vortices, the core size or radius a and the orientation of our coordinate system. The y direction, pointing from the center of the positive vortex toward the negative, we will call the spanwise direction. The direction along the core, the z direction, we will refer to as axial. The signs associated with the centers of the vortices in the figure refer to the sign of the z component of vorticity ω_z. For the orientation of the pair of counter-rotating vortices shown in the figure, the propagation by mutual advection is in the negative x direction.

The strength of a vortex is measured by its circulation Γ. The velocity induced by the each vortex outside the core of the vortex decays only as $\Gamma/2\pi r$ where r is the distance from the center of the vortex to the field point of interest. Thus the speed of descent of the dipolar pair is $c = |\Gamma|/2\pi b$ because each vortex is simply advected by the velocity field induced by the other vortex. A useful dimensional time is $\tau = 2\pi b^2/|\Gamma|$. In one period τ, the trailing vortices descend a distance of b. To add some numbers to the discussion, we could consider the wing tip vortices of a large commercial aircraft. Typical values could be taken as $b = 50$ m, $a = 5$ m, $\Gamma = 500$ m^2/s (Rennich [1]). The descent velocity would then be about 2 m/s and the period τ would be about 30 s. An approach speed of about 260 km/hr, would imply that the plane travels about 2 km in time τ, that is about 1 nautical mile. Current regulations require require about a 6 nautical mile separation, that is about 6 τ in time, following such an aircraft. This is about double the distance required between planes based on other safety considerations (Spalart [3]). Thus our goal should be to safely reduce this interval.

The maximum velocity due to a vortex of given strength or circulation Γ scales as Γ/a and occurs within the core. Thus to some extent the dangerous effects of the vortex of given strength can be decreased by increasing its core radius, which can be accomplished by turbulent diffusion. This will not however diminish the circulation and, hence, the velocity some distance from the core remains undiminished. Unfortunately, there is no simple way to decrease the circulation of the trailing vortices. Even if there was a way to reduce the strength of the vortices somewhat near the source, perhaps this is not advisable because the descent speed of the vortices would correspondingly be decreased and this is not desirable. However, if the two counter rotating vortices could be brought close together after leaving the flight path, this would be ideal. It is then possible to mix the oppositely signed vorticity from these vortices and hence cancel out the circulation by cross diffusion as mentioned above. There has been a great deal of study of instabilities of the vortex pair that would increase their interaction and hence promote cross-diffusion. One such instability is the Crow [4] instability. The effects of the Crow instability can be seen on clear days when airplanes fly at high altitudes and their contrails are visible. As the instability unfolds, the contrails merge at places to form elongated rings or loops. Although the Crow instability can lead to a decrease in Γ by cross diffusion, it appears that it proceeds too slowly and

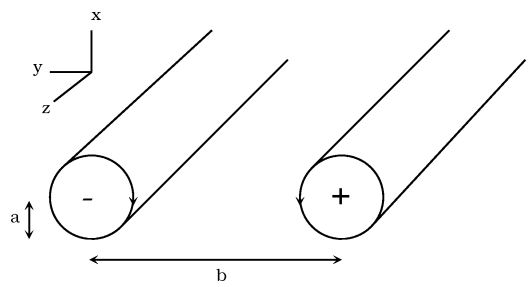

Figure 1. Schematic diagram of a pair of counter-rotating trailing vortices. In this configuration the mutual advection causes the vortices to move in the downward direction (the negative x direction). The spanwise separation of the centers of the vortices is b and the core size is a. The orientation of the axis is also displayed. Note that the z axis points out of the page.

over too long a distance to be of any use in destroying the effect of trailing vortices near airports. Recently, a great deal of attention has been directed toward a faster instability of the counter rotating vortex system called 'elliptical cooperative instability' (e.g. Leweke and Williamson [5]). The axial length scale of this instability is comparable to the vortex core size and the growth rate exceeds that of the Crow instability. The fundamental process behind this short-wavelength instability has been the subject of a number of theoretical studies (c.f. Widnall et al. [6]; Pierrehumbert [7]; Bayly [8]; Landman and Saffman [9]; and Waleffe [10]). Basically, the strain produced by one of the vortices amplifies bends in the other vortex creating a sinusoidal modulation of the core shape and position along the axial direction. The instability has been demonstrated in laboratory experiments by Thomas and Auerbach [11] and Leweke and Williamson [5]. These experiments verified many of the predictions of linear instability theory. As we will see in the next section, this instability does result in cross diffusion of vorticity and, hence, can lead to the destruction of trailing vortices. The theoretical maximum growth rate (e-folding time) of the instability is

$$\sigma = \frac{9}{8}\frac{|\Gamma|}{2\pi b^2}, \tag{1}$$

that is about $1/\tau$. Thus it would seem that the rate of growth is sufficient for our purposes. However, as we will see below, it is not clear that this instability can be initiated with sufficient strength to cause significant distortion of the vortices within the critical period of about 5τ. The contribution of the trailing vortex problem to airport delays means that the short-wave instability as it occurs now, triggered presumably by ambient turbulence, is not sufficiently strong to destroy trailing vortices on a short enough time scale. By introducing velocity perturbations in various forms, we tried to decrease the time scale of the destruction of the vortices in numerical simulations, but found the results disappointing. This will be discussed in the next section on the cooperative short-wave instability.

Our unsatisfactory results in trying to use the short wave instability to promote cross-diffusion suggested the need for a more direct forcing of the system. It turns out that if one heats the vortices, they will move closer together and descend more rapidly, both desirable effects. The idea that heating the vortices can cause them to descend more rapidly may appear counter intuitive and deserves some further explanation. A theory of this phenomenon is given by Turner [12]. The main idea is that even after the vortices are given a density different from the surrounding fluid, they will continue to propagate as a vortex pair with the propagation speed $c = |\Gamma|/2\pi b$ as given above. Let us take Γ to be the circulation of the vortex on the left (positive y) in *figure 1*. Then the propagation velocity in the (positive) x direction is

$$u = \Gamma/2\pi b \tag{2}$$

(i.e. the vortices descend if Γ is negative as in the figure). Next, we must be able to calculate the momentum of the vortex system. If the density is uniform in the z direction, then we can write

$$P_x = \iint \rho u \, \mathrm{d}x \, \mathrm{d}y, \tag{3}$$

as the x-momentum per unit length. Assuming the vortex cores have density ρ_1 while the surrounding fluid has density ρ_0, we then have the rate of change of momentum of the vortices given by the buoyancy per unit length, that is

$$\frac{\mathrm{d}P_x}{\mathrm{d}t} = -gA(\delta\rho), \tag{4}$$

where A is the cross sectional area of the buoyant fluid, $\delta\rho = \rho_1 - \rho_0$, and g is the magnitude of the acceleration of gravity. Assuming that the difference between the density inside the vortices and in the ambient fluid is

sufficiently small that it can be neglected in (3), we can then write

$$P_x = \rho_0 \iint u \, \mathrm{d}x \, \mathrm{d}y = \rho_0 \iint y\omega_z \, \mathrm{d}x \, \mathrm{d}y, \tag{5}$$

where we have used integration by parts, the definition of the vorticity $\omega_z = \partial_x v - \partial_y u$ and the fact that the velocity field of a dipole of zero net circulation falls off fast enough to remove the relevant boundary terms. Finally the model is completed by replacing the actual vortices of finite core size with line vortices of circulation Γ at $y = b/2$ and $-\Gamma$ at $y = -b/2$. Thus we obtain

$$P_x = \rho_0 \Gamma b. \tag{6}$$

Since a uniform change in temperature of the vortices will not change their net circulation, and, since the flow is incompressible, we can assume that Γ and A do not change. Substituting (6) in (4) yields

$$\frac{\mathrm{d}b}{\mathrm{d}t} = -\frac{gA}{\Gamma}\frac{\delta\rho}{\rho_0}. \tag{7}$$

Thus if $\Gamma < 0$ so that the vortices are descending, and if $\delta\rho < 0$ so that the vortices are lighter than the surrounding fluid, then they will move closer together. Integrating over time then gives

$$b = b_0 - t\frac{gA}{\Gamma}\frac{\delta\rho}{\rho_0}. \tag{8}$$

It is typical to nondimensionalize length by b, and time by τ when discussing trailing vortices. This is most useful when b is a fixed constant. Even with variable b, however, we can usefully introduce this system of nondimensionalization by referring to b_0 and τ_0, the initial values of these quantities. This system of scaling will be denoted by an asterisk superscript. Writing $b^* = b/b_0$ and $t^* = t/\tau_0$ we then have

$$b^* = 1 - \gamma t^*, \tag{9}$$

where

$$\gamma = \frac{gA\tau_0}{b_0\Gamma}\frac{\delta\rho}{\rho_0}. \tag{10}$$

From the formula for the velocity of the vortices (2), we see that the closer the vortices move together, the faster they will descend. We can use b from (8) in (2) and integrate in time to find how far the vortices move away from the flight path by a given time. The result is

$$x^* = -\left(\frac{\Gamma}{|\Gamma|}\right)\frac{1}{\gamma}\ln(1 - \gamma t^*). \tag{11}$$

Note that the sign of x^* does not depend on the sign of γ, but only on the sign of Γ, which determines the direction of the velocity. The logarithmic dependence on t may seem to indicate that the effect is weak, but *figure 2(a)* suggests otherwise. Here we have compared the descents of the neutrally buoyant and the positively buoyant vortices for values of the parameters typical of heavy commercial aircraft. We have also assumed that the difference in density between the vortex cores and the surrounding fluid is only 10%. Using the values of the relevant parameters given previously, we find $\gamma \approx 0.2$ and this was the value used in making the graphs in *figure 2*. The curves are terminated at $\tau^* = 4.5$ because at that time the separation b becomes equal to the core

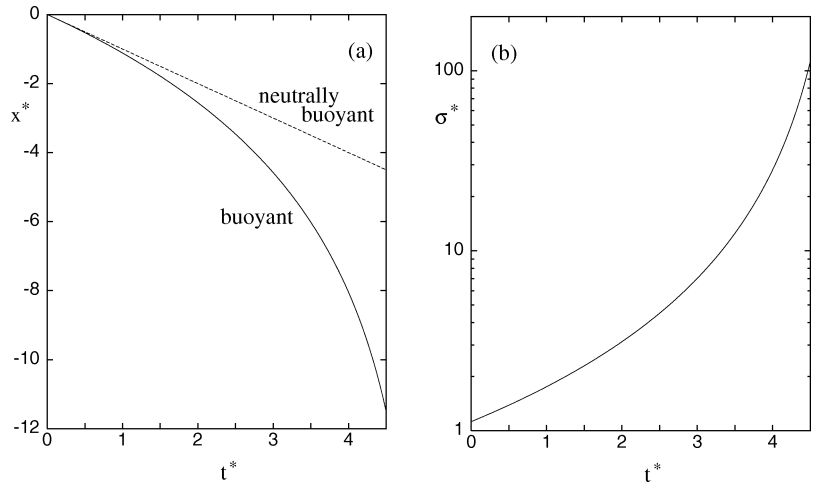

Figure 2. Graphs of the position of the trailing vortices relative to the flight path as a function of time. The position is given in units of the initial vortex separation b_0 and the time in units of $\tau_0 = 2\pi b^2/\Gamma$. In the case of neutrally buoyant vortices (dashed line) the descent speed is constant. The buoyant vortex case is shown with a solid line.

size, the vortices overlap, and the approximations that we are using are no longer valid. When the vortices are close together, they will form a compact structure like the Lamb dipole, and the simple formulas given above would have to be modified. We see from *figure 2(a)* that after one τ_0 period there is about a 10% difference between the descent distances for the neutrally buoyant and buoyant cases, but after $2\tau_0$ the difference is up to about 30% and growing. Since the period of about 5τ is relevant for the approach of heavy aircraft, the exhibited difference in trajectories is significant. More importantly, however, we note that the growth rate of the cooperative short-wave instability increases with the inverse square of the separation, so we can anticipate that this important growth rate is strongly affected by the decrease in separation. Combining (9) and (1) and writing the results in non-dimensional variables, we have

$$\sigma^* = \frac{9}{8}(b^*)^{-2} = \frac{9}{8}(1 - \gamma t^*)^{-2}. \tag{12}$$

We see in *figure 2(b)* that a change in density of just 10% can result in a near doubling of the instability growth rate by time τ_0, tripling by time $2\tau_0$, and a 25 fold increase by time 4τ. Thus, the thermal effect of Turner [12] can enhance the growth rate of the short-wave instability to such a level as to make it a method worth considering.

In the next section, we will show some results from three-dimensional simulations suggesting that it may be difficult to mechanically enhance the effects of the short-wave instability to the point that it would be useful in destroying trailing vortices in practical situations. Then in section 3, we will show some evidence from three-dimensional simulations that the Turner effect may produce the desired enhancement. Finally, some practical considerations for actually employing this method for destroying trailing vortices are discussed in the conclusion section.

2. Pure short-wave instability

We base our study of the fundamental short-wave instability with no thermal effects on the Navier–Stokes equations for a uniform-density incompressible fluid. Our numerical model solves the momentum equation

which can be written as

$$\frac{\partial u_i}{\partial t} + \frac{\partial u_i u_j}{\partial x_j} = -\frac{\partial p}{\partial x_i} + \nu \frac{\partial^2 u_i}{\partial {x_j}^2}, \tag{13}$$

with $\nabla \cdot \mathbf{u} = 0$. The numerical scheme uses a staggered mesh with the velocity components located on the faces of the cell and the pressure at the center, and a fractional step method in time (Kim and Moin [13]). Although we would like to simulate the high Reynolds number flows appropriate to large aircraft, this is not possible with the computing resources available. In all the simulations that we will discuss below, the Reynolds number, based on the vortex strength, $Re = \Gamma/\nu$ was taken to be 3400.

The choice of the structure of the initial vortices requires some care. If one starts with vortices whose vorticity distributions in an x–y cross section are radially symmetric, then there will be a transition period in which fluid is shed in the wake of the vortices during the period in which the structure of each vortex adjusts to the presence of the other vortex. This adjustment is a purely two-dimensional process (cf. Carnevale and Kloosterziel [14]) and is of little interest to the present study. We could wait for this adjustment period to pass and then use the resulting adjusted vortices as the initial vortices for our study. As an alternate approach, we found that the adjustment phase could be mostly eliminated by using vortices whose structure is given by the analytical formula for the vortices of the Lamb dipole (Lamb [15], section 165). This is a vortex structure in which there are two counter-rotating vortices with the entire dipolar vorticity distribution confined in a circular region whose radius we will denote by $a_{\mathcal{L}}$. When unperturbed, the Lamb dipole propagates at a constant speed $U_{\mathcal{L}}$ without change. For sufficiently high resolution, the form-preserving motion of the Lamb dipole can be readily simulated. Taking as an initial condition the two semicircular halves of the Lamb dipole separated by some distance, we found that in the subsequent evolution the two vortices adjusted more smoothly and without the large amount of vorticity shedding observed in the case initialized with two circularly symmetric vortices. In all of the simulations presented below, the unperturbed basic state is taken as the two halves of the Lamb dipole with the vorticity extrema separated by some distance, and the initial condition is prepared by adding perturbations to this.

A system of units that will be useful here is the advective time scaling based on the unperturbed Lamb dipole with zero separation between the halves of the Lamb dipole. The unit of length in this system is $a_{\mathcal{L}}$ and the time unit is $a_{\mathcal{L}}/U_{\mathcal{L}}$. All quantities without the asterisk superscript will be in these units. The theoretical speed of the unperturbed dipole in units of b_0 and τ_0 is approximately $c^* = 0.87$ (cf. Kloosterziel et al. [16]).

In one series of simulations, we initialized the flow by adding a perturbation that was a randomly generated three-dimensional velocity field. This perturbation was localized to the region were the axial vorticity ω_{z0} was greater in magnitude than a given threshold (set arbitrarily at 20% of the unperturbed vorticity maximum). The random velocity thus generated was not solenoidal, but this defect was remedied automatically by the first time step of the simulation which projects the initial velocity onto a solenoidal field. The perturbed field is then found to have pointwise fluctuations in the cross vorticity components, ω_x and ω_y of at most 20% of $|\omega_{z0}|_{\max}$. The basic simulation consisted of the interaction of the pair of the counter-rotating vortices for a fixed period of time. Three different values were used for the separation between the vortices. By running experiments at different resolutions and with different domain sizes, we found a representation of the short-wave instability that compared very well with the laboratory results (Leweke and Williamson [5]) for the short-wave instability when we set the number of grid points in each direction as $(N_x, N_y, N_z) = (128, 192, 128)$ and set the domain size as $(L_x, L_y, L_z) = (2\pi, 3\pi, \pi)$. The value of L_z was chosen to allow two full wavelengths of the fastest growing mode of the instability. This choice of domain size will be discussed further below.

We performed three simulations with different values of b. The circulation was the same in each case: $\Gamma = 6.83$. The values of b were measured a short time after the initial adjustment of the dipole. In units of

$a_{\mathcal{L}}$ the values of b were 1.0, 1.4 and 1.9. There are various quantities that can be used to measure the progress of the cooperative instability. For the unperturbed pair of vortices, the only nonzero component of the vorticity is the axial vorticity ω_z. Thus a good indicator of the growth of an instability would be the evolution of the maximum value of the magnitude of one of the other components of vorticity. In *figure 3(a)*, we plot the evolution of the maximum value of the spanwise vorticity ω_y for the three simulations with different values of b. Vorticity and time have been nondimensionalized using τ as defined above. Also plotted is the history of the maximum value of the axial vorticity (chain-dashed line) for one of the simulations. The curves for ω_y each have a section that is roughly linear on this linear-logarithmic plot, indicating exponential growth in time. Based on theoretical arguments, Leweke and Williamson [5] predict $\sigma^* = 9/8$ for the growth rate of the cooperative instability. This is based on an assumption that the separation b is large and the flow is inviscid. In the simulations reported here, the separation b was taken as the initial distance between the vorticity extrema. The growth rate for the largest separation case ($b = 1.9$) is found to be approximately 0.9. Viscous corrections to the growth rate for this value of b give a theoretical growth rate of $\sigma^* = 0.96$. This is the closest match that we have, and the discrepancy between theory and simulation is larger for the smaller values of b. The variation in the growth rate with b is not entirely accounted for by viscous effects and may indicate that our values of b are not sufficiently large to apply the theoretical arguments without modification, but increasing the separation while continuing to resolve all the features of the short-wave instability was beyond our resources.

Note that in *figure 3(a)* the value of ω_y becomes comparable to ω_z for $t^* \approx 13$. The evolution of ω_x (not shown) is similar to that of ω_y. The vorticity components in x and y directions becoming comparable in magnitude to the axial vorticity indicates that the dipolar structure of the vortices is breaking down. As we will see, the ω_x and ω_y components produce strong deformations associated with small scales as would occur in a transition to turbulent flow. One indication of the destruction of the vortices is the history of the circulation which is shown in *figure 3(b)*. This circulation Γ was obtained by integrating the axial vorticity in each xy plane for $-L_y/2 \leqslant y \leqslant 0$, and then averaging over z. By $t^* \approx 13$, in all cases, there is a significant drop in Γ and this occurs at approximately the same time that the values of ω_x and ω_y become comparable to that of ω_z.

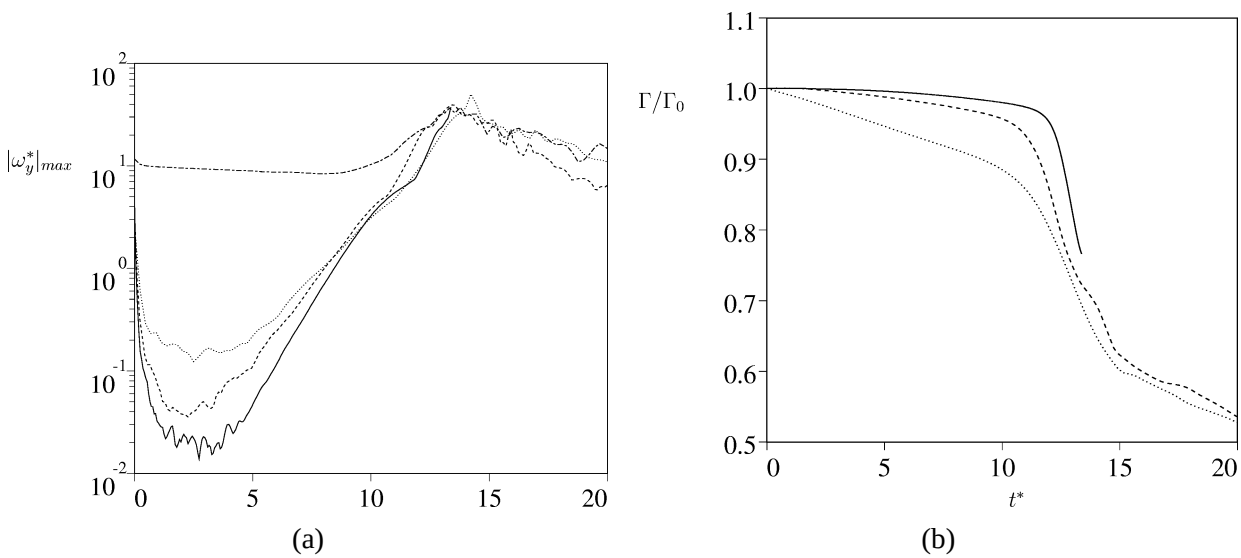

Figure 3. (a) History of the maximum value of the spanwise vorticity ω_y for three cases: solid $b = 1.9$, dashed $b + 1.4$ and dotted $b = 1.0$. For comparison, the history of the maximum value of ω_z (chain dashed) for $b = 1$ is also plotted; (b) history of the circulation normalized by its initial value. The line types for the different values of b are as in panel (a).

To visualize the three dimensional character of the short-wave instability, we produced isosurface plots of vorticity. Visualization by this method shows some structures that are very similar to those observed by dye visualization in the experiments by Leweke and Williamson [5]. For each of the three simulations with different values of b the vorticity structures observed were qualitatively similar at the same times when time was scaled with τ. In *figure 4*, we show the isosurface plots of the magnitude of the vorticity $|\omega|$ for the case $b = 1.9$. The isosurface value is the same at each time shown and is $|\omega/\omega_0| = 0.4$ where $|\omega_0|$ is the maximum magnitude of the unperturbed dipole vorticity field. In both the laboratory experiments and the simulations the sinusoidal bending of the vortex cores is in phase, that is the instability is sinuous. This is interesting because when the effect of one vortex upon the other is modeled as pure strain, there is no mechanism for choosing the phase relationship between the distortions of each vortex. The isosurface plot for $t^* = 9.0$ in *figure 4* represents the field at a time in the exponentially growing phase of the instability (cf. *figure 3(a)*). We compared the perturbation vorticity and velocity fields at this point in the evolution to the predictions of linear theory based on Rankine (top-hat profile) vortices and the match was very good. By time $t^* = 10.5$, nonlinear effects are evident. The formation of 'caps' on the points where the isosurface is most curved results from vortex stretching in the spanwise direction. This is followed by the production of the vortices seen at $t^* = 12.0$ which span the two original cores and which begin the cross-diffusion of circulation.

As for the wavelength of the fastest growing mode, theory based on a Rankine vortex (uniform vorticity core) predicts a wavelength $\lambda = 2.51a_R$, where a_R is the radius of the core. Unfortunately, since our vortices are not

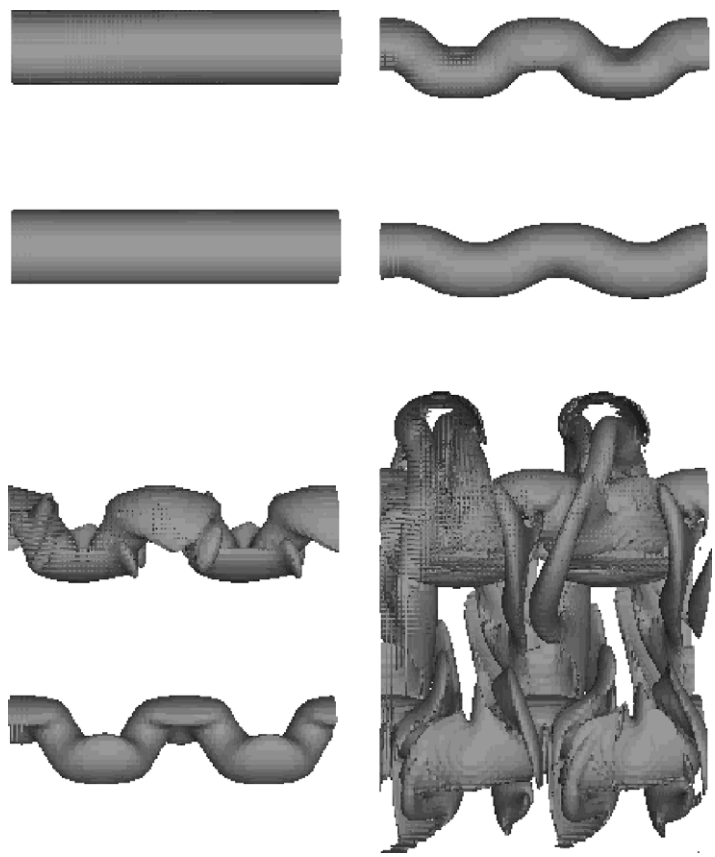

Figure 4. Isosurface plots of $|\omega/\omega_0| = 0.4$ for the case of the two vortices separated by $b = 1.9$. The times represented from left to right, top to bottom, are $t^* = 1.5$, 9.0, 10.5 and 12.0.

circularly symmetric in cross section and do not have a uniform distribution of ω_z, it is not clear what distance should be used for a_R in making a comparison with the theory. Since the Rankine vortex achieves its maximum vorticity at the radial position a_R, we can try to substitute for this the radius where the maximum value of velocity is achieved along some radial direction. At $t_* = 9.0$, for the case $b = 1.9$ shown in *figure 4*, the distance between the points of minimum and maximum v_y for one of the vortices is approximately $0.69a_{\mathcal{L}}$. Substituting this value for a_R, the wavelength of the fastest growing mode should be $\lambda = 1.73a_{\mathcal{L}}$. In the simulation we found $\lambda = 0.5\pi a_{\mathcal{L}} \approx 1.57a_{\mathcal{L}}$, which is within about 10% of the predicted value. The possible wavelengths in the periodic domain are discrete and the instability cannot pick out a wavelength that is not one of the discrete set. We varied L_z over a large range of values, sufficiently large to observe the transition to both one and three full wavelengths within our domain. We found that variations of L_z by 10% from the value that we chose did not change the growth rate appreciably, while variations just beyond this did produce slower growth rates. Thus we were satisfied that $L_z = \pi a_{\mathcal{L}}$ was a reasonable choice choice for the domain size.

From a practical standpoint, *figure 3(a)* suggests that random perturbations applied to the vortices is an inefficient way to initiate the cooperative instability. The initial perturbation has maximum vorticity amplitude of about 20% that of the unperturbed vortices. However, this amplitude decays greatly in the initial transient period, and the larger the value of b, the lower the value reached in this initial decay. It took about 5τ for the exponential growth of the unstable modes to become evident. It appears that much of the initial perturbation is composed of decaying modes. The small proportion originally in growing modes eventually amplifies and dominates, but this appears to be a relatively long process for our purposes. If the perturbation could be applied purely in the fastest growing normal mode, then, theoretically, the transient phase could be avoided. With an inviscid theoretical maximum growth rate of $\sigma^* = 9/8$, the period of growth would only need to be about 2τ to begin the destruction of the vortices. We attempted to initialize the flow field with the dipole perturbed by the fastest growing eigenmode predicted by theory based on the Rankine vortex in a pure strain field (Leweke and Williamson [5], Orlandi et al. [17]). This reduces the transient period by about half but still leaves a significant period of decay and a period of about 9τ is still required for the destruction of the circulation to start. Given that our initial vortices are not Rankine vortices and that there is a distortion of each vortex due to the presence of the other, it is not surprising that the theoretical normal mode based on the Rankine vortex in a pure strain field is not a pure growing normal mode for the actual dipole. This result tends to suggest that it would be necessary for the initial perturbation to very closely approximate the form of the fastest growing mode in order to excite this mode to significant levels within a few τ. This seems impractical from the viewpoint of aircraft design. Therefore, we turn to thermal forcing and the Turner effect as an alternate approach to the problem.

3. Thermal forcing of trailing vortices

The simplest approximation that includes the buoyancy force due to small density variations is the Boussinesq approximation. If the acceleration of gravity is taken to be in the negative x-direction, which is the direction of our dipole motion, then the Boussinesq approximation for the momentum equation can be written as

$$\frac{\partial u_i}{\partial t} + \frac{\partial u_i u_j}{\partial x_j} = -\frac{\partial p'}{\partial x_i} + \frac{1}{Re}\frac{\partial^2 u_i}{\partial {x_j}^2} - \theta\delta_{i1}, \tag{14}$$

and the equation for the density is

$$\frac{\partial \theta}{\partial t} + \frac{\partial \theta u_j}{\partial x_j} = +\frac{1}{RePr}\frac{\partial^2 \theta}{\partial {x_j}^2}. \tag{15}$$

This notation assumes the directions x, y, z are numbered sequentially from 1 to 3, and δ_{ij} is the Kronecker delta. These equations are nondimensionalized using length $a_{\mathcal{L}}$ and time $a_{\mathcal{L}}/U_{\mathcal{L}}$. The dimensionless density θ is given by

$$\theta = \frac{\rho' g a_{\mathcal{L}}}{\rho_0 U_{\mathcal{L}}^2}, \tag{16}$$

where ρ' is the perturbation to the background density ρ_0, and g is the acceleration of gravity. Note that p' is the pressure less the background pressure $-\rho_0 g x$. The Reynolds number is given by $Re = U_{\mathcal{L}} a_{\mathcal{L}}/\nu$, and Pr is the Prandtl number given by $Pr = \nu/\kappa$ where κ is the thermal diffusivity.

In deriving the Boussinesq approximation, various terms are neglected under the assumption that ρ'/ρ is sufficiently small. In particular, a term equal to

$$\left(\frac{\rho'}{\rho}\right)\left(\frac{1}{\rho_0}\frac{\partial p'}{\partial x}\right)$$

has been neglected. The Boussinesq approximation is strictly valid only if this term is small compared to the retained term θ. This can be translated into the statement that the centripetal acceleration within the trailing vortex, which is on the order of U^2/a, should be much less than the acceleration due to gravity. Assuming a vortex circulation of 100 m^2/s and a core radius of about 5 m would make the ratio of centripetal to gravitational acceleration about 1/2. So, our simulations with $\Gamma = 100$ m^2/s case, a value typical of medium sized jet aircraft, are probably at the extreme limits of the validity of the Boussinesq approximation, and simulation with the full Navier–Stokes equations should be performed in the future to verify the results obtained here. For the stronger circulation typical of the heavy commercial aircraft discussed in the introduction, it would certainly be necessary to use the full Navier–Stokes equations for accurate predications, but, hopefully, our simpler Boussinesq simulations will provide some first insights into the effect of thermal forcing.

To see how buoyancy forcing affects a pair of counter-rotating vortices, we began with a simple test. We used the same basic vortex pair as in the previous section. To these vortices we added an initial distribution of θ that was taken to be independent of the axial coordinate z, and proportional to the magnitude of the vorticity in each of the vortices with the maximum amplitude set at θ_0. In one case we took $\theta_0 = +1$ and in the other $\theta_0 = -1$. Since there was no variation in the axial direction, two-dimensional numerical simulations sufficed to show the evolution. In *figure 5*, where we have plotted the trajectories of the extrema of vorticity for these two simulations, we see the interesting effect of the temperature perturbation. As predicted in the introduction, the speed of the 'heavy' vortices decreases, and the separation of the vortices increases, while the 'light' vortices move closer together and their rate of descent increases.

To translate the nondimensional values of θ used here into physical values, we have recourse to order of magnitude estimates. First we estimate the values to use for $a_{\mathcal{L}}$ and $U_{\mathcal{L}}$ in formula (16). The radius of the vortices in the unperturbed Lamb dipole cannot be related easily to the radius of actual trailing vortices. In the case of the dipole with $b = 1.9$, we found a maximum velocity at a distance of about $0.7a_{\mathcal{L}}$ from the center of the vortex. Thus if we take a core radius for a trailing vortex as $a = 5$ m, then we would estimate $a_{\mathcal{L}}$ to be somewhat larger, say $a_{\mathcal{L}} = a/0.7 \approx 7$ m. The speed $U_{\mathcal{L}}$ of a Lamb dipole in terms of the circulation of its vortices and $a_{\mathcal{L}}$ is given approximately by $U_{\mathcal{L}} = \Gamma/(2.2\pi a_{\mathcal{L}})$ (see Carnevale and Kloosterziel [14]). With $\Gamma = 100$ m^2/s, this would give $U_{\mathcal{L}} \approx 2$ m/s. Thus for $|\theta_0| = 1$ the magnitude of the density variation as a percentage of the background would be 6% according to formula (16). In terms of temperature, this would correspond to about a 20° variation on a background of 300°K.

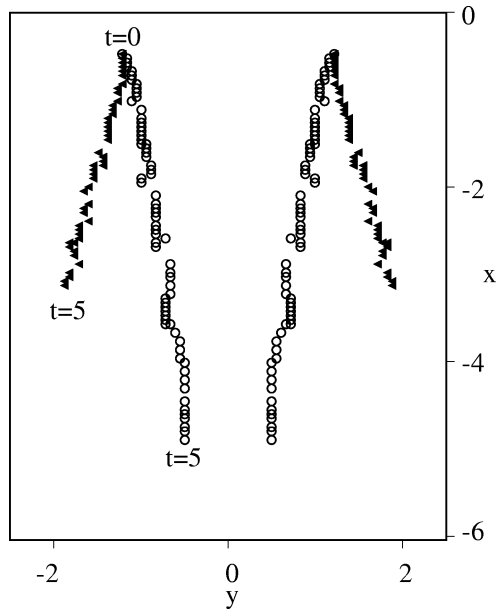

Figure 5. Trajectories of the vorticity extrema for $\theta_0 = -1$ (open circles) and $\theta_0 = +1$ (solid triangles). The vortices propagate in the negative x-direction. The total period of time represented is 5 in advective time units. The symbols represent positions taken at time intervals of 0.1.

It is interesting to consider how the temperature variation forces the growth of the non-axial vorticity. Taking the curl of the momentum equation, we obtain the vorticity equation,

$$\frac{\partial \omega_i}{\partial t} + u_j \frac{\partial \omega_i}{\partial x_j} = \omega_j \frac{\partial u_i}{\partial x_j} + \frac{1}{Re} \frac{\partial^2 \omega_i}{\partial {x_j}^2} - \varepsilon_{ij1} \frac{\partial \theta}{\partial x_j}, \tag{17}$$

from which we can see how the buoyancy term directly forces the vorticity components ω_y and ω_z. In particular, a modulation of θ in the z direction will directly force the growth of ω_y, which is the field that we used to monitor the progress of the cooperative instability in the random initial velocity perturbation cases. There we found that when ω_y became comparable to ω_z, strong cross diffusion between the counter-rotating vortices occurred. Thus if we can accelerate the growth of ω_y by modulating θ in the axial direction, we may achieve a more rapid destruction of the coherent vortices. Since the rate of growth of ω_y will be directly proportional to $\partial\theta/\partial z$ we can expect that the early growth will be linear in time. If $\partial\theta/\partial z$ is sufficiently large, this linear growth can dominate the exponential growth of an eigenmode perturbation of the cooperative instability.

Hoping to combine the effects of both temperature forcing and the cooperative instability, we decided to modulate the temperature field with the same wavelength that was observed to be the wavelength of the fastest growing mode in the experiments with random initial velocity perturbations. Restricting ourselves to a density perturbation that is everywhere negative, as may be achieved by heating, we chose to modulate the density in the axial direction by multiplying our original perturbation described above with a factor given by $0.5(1 - \sin(k_\theta 2\pi z/L_z))$. With $L_z = \pi a_{\mathcal{L}}$, the appropriate wavenumber is $k_\theta = 2$. We performed a series of simulations with different amplitudes for θ_0 (the maximum value of the initial perturbation). For $\theta_0 = -1$, we found that the values of $|\omega_y|_{\max}$ grew to the same levels as in the random perturbations cases but in a much shorter time. This is shown in *figure 6*, where we plot the results for the same three values of the separation b as used in the previous simulations. For comparison, we also plot the results from the runs described in the previous section where the only perturbation was the random velocity perturbation. The time scale is in τ_0 units.

Thus, we see that for θ_0, levels of $|\omega_y|_{\max}$ sufficient to destroy the coherence of the vortices are reached in a period of a few τ_0 units. Also, it is encouraging that as the distance b between the vortices increases, the time at which the peak in $|\omega_y|_{\max}$ is reached decreases.

In *figure 7*, we show the evolution of an isosurface of vorticity magnitude of the thermally perturbed vortex pair for the case $b = 1.9$, $\theta_0 = -1$. Note that since the vortices will be drawn together where the density is lowest, and since temperature is distributed with the same phase on each vortex, the pair is forced into the varicose mode. Recall that in the case of the random velocity perturbations, the fastest growing mode was sinuous. This suggests that it may be possible to increase the growth rate of the instability by shifting the phase of the temperature on one vortex relative to the other in the temperature modulation in the axial direction. We performed two additional simulations, with phase shifts $\alpha = \pi/8$ and $\pi/4$. The resulting graphs of the evolution of $|\omega_y|_{\max}$ are shown in *figure 8(a)* along with the graph for the $\alpha = 0$ case. Although there does not appear to be much difference in the growth during the early phase, which is dominated by buoyancy forcing, ultimately the shift by $\pi/4$ does yield an increase in the peak amplitude by a factor greater than 2. Thus it seems that the phase shift does enhance the growth in the period of the evolution that we suppose to be dominated by cooperative instability. *Figure 8(b)* shows the history of Γ which is calculated by summing all of the axial vorticity separately for $y < 0$. This shows that the introduction of the phase shift causes the circulation to decay earlier and more rapidly. Unfortunately, it does not seem possible to force the two vortices into a sinuous mode by using heating alone.

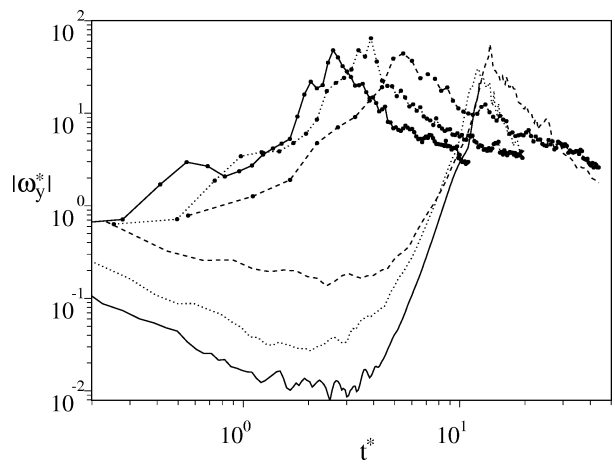

Figure 6. History of $|\omega_y|_{\max}$ for the dipoles separated by $b = 1.9$ solid, dotted $b = 1.4$ and $b = 1$ dashed. The curves without symbols correspond to the cases perturbed initially with the random velocity field, while those with circles correspond to the cases initially perturbed with spatially-periodic density variations ($\theta_0 = -1$).

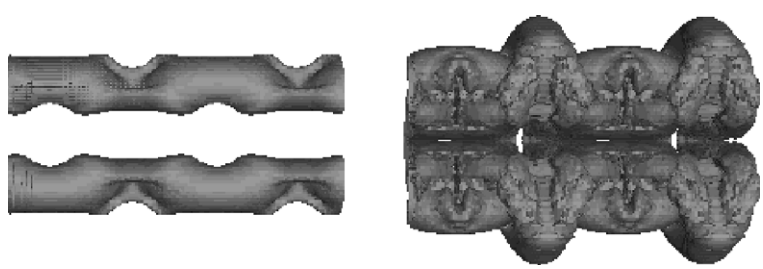

Figure 7. Plots of the isosurface $|\omega|/\omega_0 = 0.64$ at $t^* = 1$ (left) and $t^* = 2$ (right).

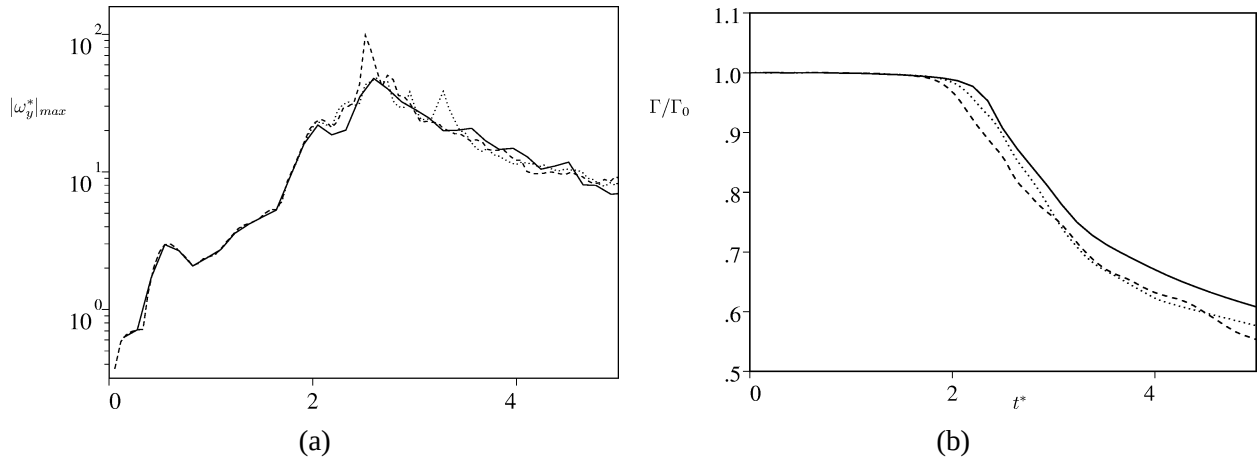

Figure 8. History of (a) spanwise vorticity and (b) circulation for solid $\alpha = 0$, dotted $\alpha = \pi/8$ and dashed $\alpha = \pi/4$.

4. Conclusions

We have obtained some encouraging results that suggest thermal forcing may be useful in promoting both the rapid departure of vortices from a flight path and the acceleration of short-wave instabilities that can lead to the destruction of the vortices through cross-diffusion. Our work is only preliminary since it was limited by available computational resources to deal with only short spans b and relatively moderate vortex strength Γ. We already mentioned above that for the thermal forcing problem, our Boussinesq code is not well suited for dealing with $\Gamma \approx 500$ m^2/s and hence we restricted ourselves to the $\Gamma \approx 100$ m^2/s case. To go to stronger vortices would require solving the full Navier Stokes equations. As for the limitation on b, typical wing spans for heavy aircraft are such that $b/a \approx 12$ while here we have reported only values up to 1.9. It is tempting to push beyond this limit. We did perform runs with somewhat larger values of b, but with DNS there are some fundamental limitations. In particular, the dependence of instability growth rates on viscosity becomes an issue. Up to this point we have not discussed the role of viscosity in determining the growth rate of the short-wave instability. For real flight situations, the Reynolds number is sufficiently high that this effect is not of concern. However, in our simulations we must keep a relatively low Reynolds number to avoid numerical instabilities and inaccuracies. For a finite Reynolds number a theoretical prediction for the short-wave instability growth rate is (cf. Leweke and Williamson [5])

$$\sigma = \frac{9}{8}\frac{\Gamma}{2\pi b^2} - \nu k_0^2, \tag{18}$$

where k_0 is the wavenumber of the fastest growing mode, which is approximately given by $k_0 \approx \pi/a$. Thus, for b sufficiently large, viscous decay will inhibit the instability significantly. Using the Reynolds number defined by the vortex strength, we see from (18) that the Reynolds number should be much smaller than about $55(b/a)^2$. Thus with our Reynolds number set at 3400, as in the simulations discussed above, viscous effects would not be significant for b/a up to about 2.5. Also as b is increased, the size of the domain and, hence, the number of grid points must be increased. Using the DNS method in a simulation with $b/a = 12$ while resolving all relevant scales would be prohibitively expensive in computer resources and is left for future investigations.

As for the practicality of using density perturbations, we can say a few words here. We imagine that the method of producing the density variation for aircraft trailing vortices would be by heating within the vortices. This could be accomplished either by redirecting and modulating the existing jet exhaust or by adding auxiliary burners in the vicinity of the points where the vortices roll up (e.g. wing tips, and flap edges). This heating

would only be required during takeoffs and landings. Consider the problem of modulating the temperature of a vortex with a sinusoidal perturbation of wavelength about twice the vortex core radius with an amplitude 30°C over say a distance of 10 km. If we take the estimates of $a = 5$ m for the core radius and 300 km/hr for the plane speed, we calculate that the total amount of Kerosene that would need to be burned to produce such a perturbation would be only about 140 kg. This would seem a reasonable cost if the result were to substantially minimize the effect of the trailing vortices.

To conclude, let us say that although our preliminary results indicate that the Turner [12] effect is a good candidate for alleviating the problems of trailing vortices, it will require a substantial modeling effort to see if these ideas will scale up to stronger vortices with larger separations. Alternatively, we may suggest that a more efficient way of proceeding at this point may be through laboratory experiments.

Acknowledgments

The authors gratefully acknowledge the important contribution of W.C. Reynolds in suggesting the use of temperature perturbations to drive the instability of the vortices. The authors are very grateful to the Center for Turbulence Research for making their collaboration possible. GFC and PO received additional support from the National Science Foundation (INT-9511552) and the Office of Naval Research (N00014-97-1-0095). In addition, GFC acknowledges support from the San Diego Supercomputer Center under an NPACI award.

References

[1] Rennich S.C., Accelerated destruction of aircraft wake vortices, Report, Dept. Aeronautics and Astronautics, TR SUDAAR 705, Stanford University, Stanford, CA, USA, 1997.
[2] Orlandi P., Vortex dipole rebound from a wall, Phys. Fluids A 2 (8) (1990) 1429–1436.
[3] Spalart P.R., Airplane trailing vortices, Annu. Rev. Fluid Mech. 30 (1998) 107–138.
[4] Crow S.C., Stability theory for a pair of trailing vortices, AIAA J. 8 (1970) 2172–2179.
[5] Leweke T., Williamson C.H.K., Cooperative elliptic instability of a vortex pair, J. Fluid Mech. 360 (1998) 85–119.
[6] Widnall S.E., Bliss D.B., Chon-Yin Tsai, The instability of short waves on a vortex ring, J. Fluid Mech. 66 (1974) 35–47.
[7] Pierrehumbert R.T., Universal short-wave instability of two-dimensional eddies in an inviscid fluid, Phys. Rev. Lett. 57 (1986) 2157–2159.
[8] Bayly B.J., Three-dimensional instability of elliptical flow, Phys. Rev. Lett. 57 (1986) 2160–2163.
[9] Landman M.J., Saffman P.G., The three-dimensional instability of strained vortices in a viscous fluid, Phys. Fluids 30 (1987) 2339–2342.
[10] Waleffe F., On the three-dimensional instability of strained vortices, Phys. Fluids 2 (1990) 76–80.
[11] Thomas P.J., Auerbach D., The observation of the simultaneous development of a long- and a short-wave instability mode on a vortex pair, J. Fluid Mech. 265 (1994) 289–302.
[12] Turner J.S., A comparison between buoyant vortex rings and vortex pairs, J. Fluid Mech. 7 (1959) 419–432.
[13] Kim J., Moin P., Application of a fractional-step method to incompressible Navier–Stokes equations, J. Comput. Phys. 59 (1985) 308–323.
[14] Carnevale G.F., Kloosterziel R.C., Lobe shedding from propagating vortices, Physica D 76 (1994) 147–167.
[15] Lamb H., Hydrodynamics, Dover, New York, 1945.
[16] Kloosterziel R.C., Carnevale G.F., Philippe D., Propagation of barotropic dipoles over topography in a rotating tank, Dynam. Atmos. Oceans 19 (1993) 65–100.
[17] Orlandi P., Carnevale G.F., Lele S.K., Shariff K., DNS study of stability of trailing vortices, in: Proceedings of the 1998 Summer Program, Center for Turbulence Research, NASA Ames, Stanford University, 1998, pp. 187–208.